# Supporting Information

## Interaction Between Encapsulated Excited Organic Molecules and Free Nitroxides: Communication Across a Molecular Wall

Mintu Porel,[a] Steffen Jockusch,[b] M. Francesca Ottaviani,[c] N. J. Turro[b] and V. Ramamurthy[a]

[a]Department of Chemistry, University of Miami, Coral Gables, FL, 33124, USA

[b] Department of Chemistry, Columbia University, New York, NY 10027, USA

[c] Department of Earth, Life and Environmental Sciences (DiSteVA) University of Urbino, Campus ex-Sogesta, Loc. Crocicchia, 61029 Urbino, Italy

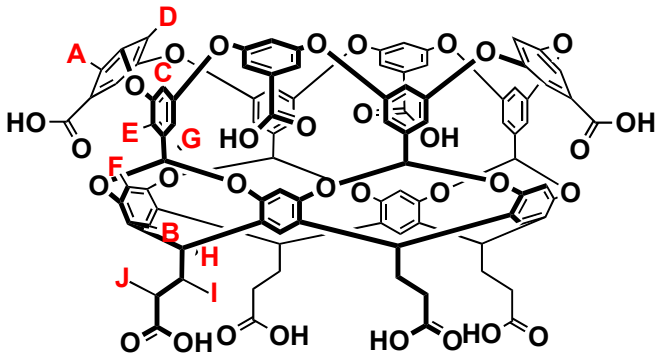


octa acid (OA)

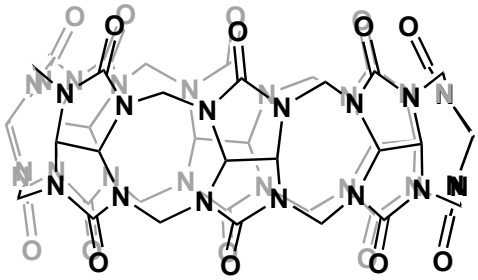

cucurbit[8]uril (CB8)

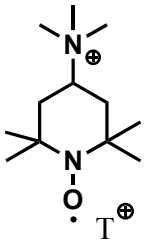

T⊕

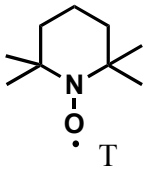

T

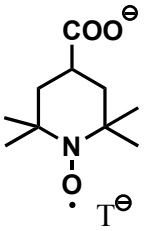


T⊖

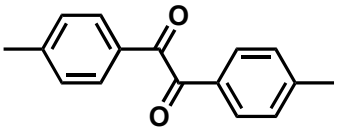

4,4'-dimethyl benzil (**1**)

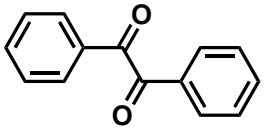

benzil (**2**)

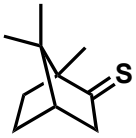

camphorthione (**3**)

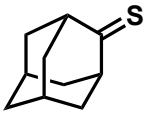

adamantanethione (**4**)

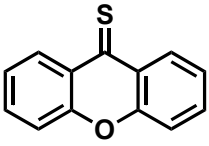

xanthione (**5**)

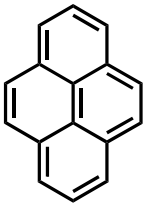

pyrene (**6**)

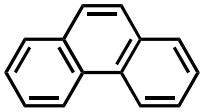

phenanthrene (**7**)

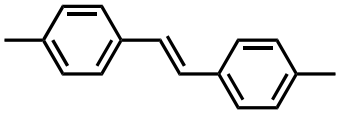

4,4'-dimethylstilbene (**8**)

**Scheme S1**. Structure of hosts and guests examined in this study. The letters "A" to "J" in OA represent the corresponding protons.

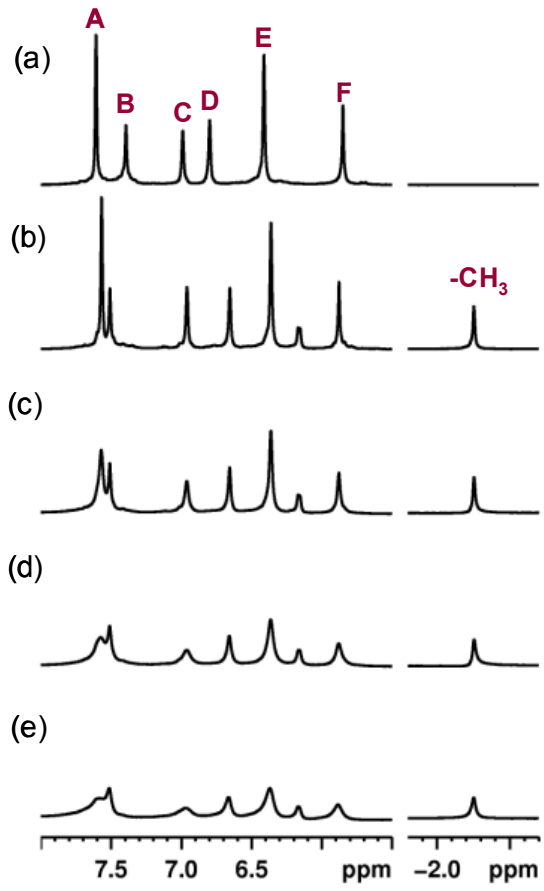


**Figure S1**. $^{1}$H NMR spectra (500 MHz, $D_2O$) of (a) OA, (b) **1**/OA(1:2), (c) **1**/OA/$\mathbf{T}^{\oplus}$ (1:2:1), (d) **1**/OA/$\mathbf{T}^{\oplus}$ (1:2:2), (e) **1**/OA/$\mathbf{T}^{\oplus}$ (1:2:3). [**1**] = 0.5 mM, [OA] = 1 mM and [$\mathbf{T}^{\oplus}$] = 0.5 mM to 1.5 mM in 10 mM borate buffered $D_2O$.

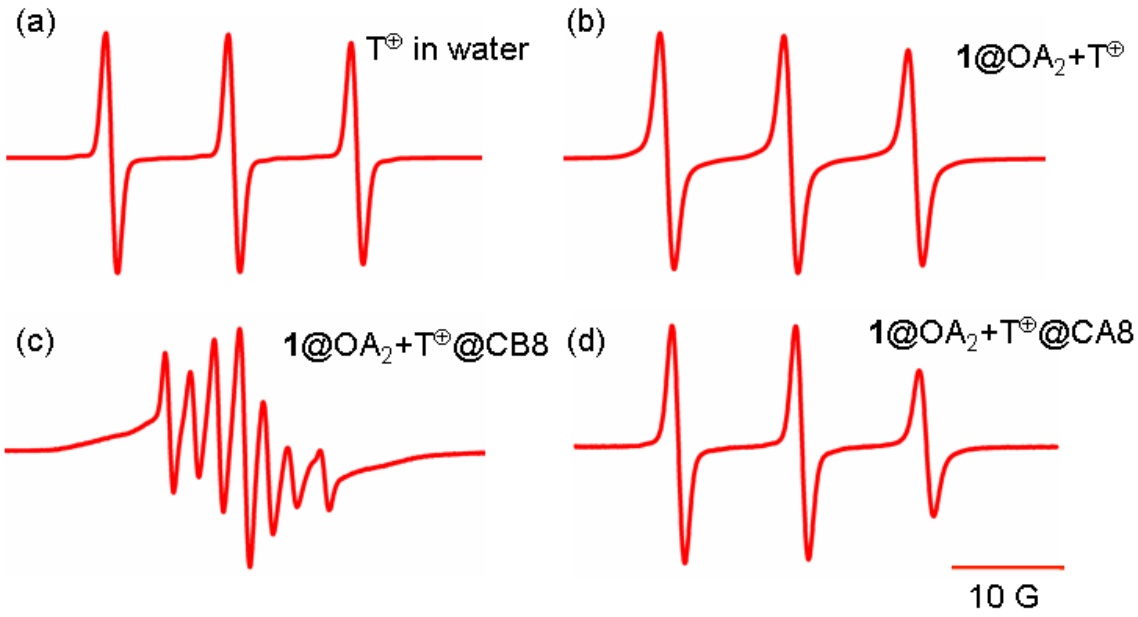


**Figure S2**. EPR spectra of (a) $\mathbf{T}^{\oplus}$ in water ($\tau_c$ = 0.02 ns, $A_N$ = 16.8 G), (b) **1**/OA/$\mathbf{T}^{\oplus}$ (1:2:2; $\tau_c$ = 0.05 ns, $A_N$ = 16.7 G), (c) **1**/OA/$\mathbf{T}^{\oplus}$/CB8 (1:2:2:2) and (d) **1**/OA/$\mathbf{T}^{\oplus}$/CA8 (1:2:2:2; $\tau_c$ = 0.14 ns, $A_N$ = 16.7 G); [**1**] = 0.5 mM, [OA] = 1 mM, [$\mathbf{T}^{\oplus}$] = 1 mM, [CB8] = 1 mM and [CA8] = 1 mM in 10 mM borate buffered $H_2O$.

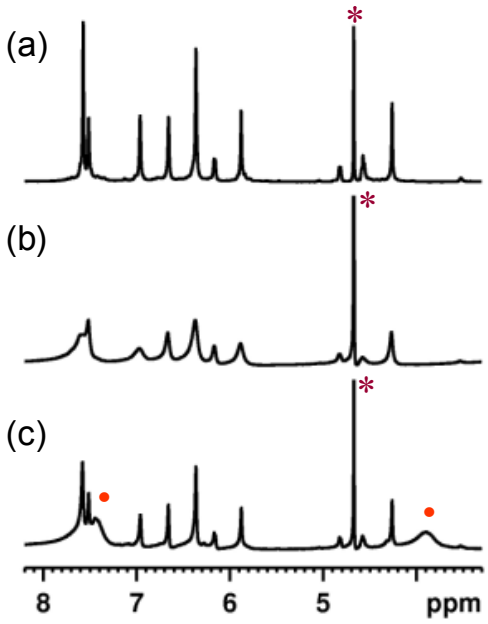


**Figure S3**. $^{1}$H NMR spectra (500 MHz, $D_2O$) of (a) **1**/OA (1:2) , (b) **1**/OA/$\mathbf{T}^{\oplus}$ (1:2:2), (c) **1**/OA/ $\mathbf{T}^{\oplus}$/CA8 (1:2:2:2), [**1**]=0.5 mM, [OA] = 1 mM, [$\mathbf{T}^{\oplus}$] = 1 mM and [CA8] = 1 mM in 10 mM borate buffered $D_2O$, "•" represents CA8 proton resonances, "*" represents residual $H_2O$ proton resonances.

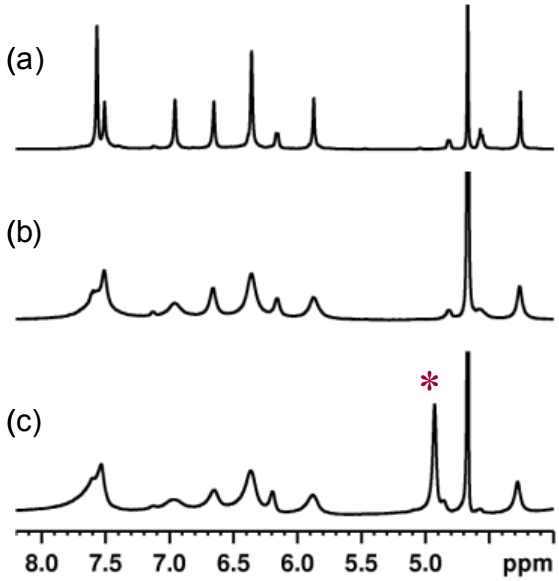


**Figure S4**. $^{1}$H NMR spectra (500 MHz, $D_2O$) of (a) **1**/OA (1:2), (b) **1**/OA/ $\mathbf{T}^{\oplus}$ (1:2:2) and (c) **1**/OA/$\mathbf{T}^{\oplus}$/γ-CD (1:2:2:2), [**1**]=0.5 mM, [OA] = 1 mM, [$\mathbf{T}^{\oplus}$] = 1 mM and [γ-CD] = 1 mM in 10 mM borate buffered $D_2O$, "*" represents γ-CD proton NMR signal.

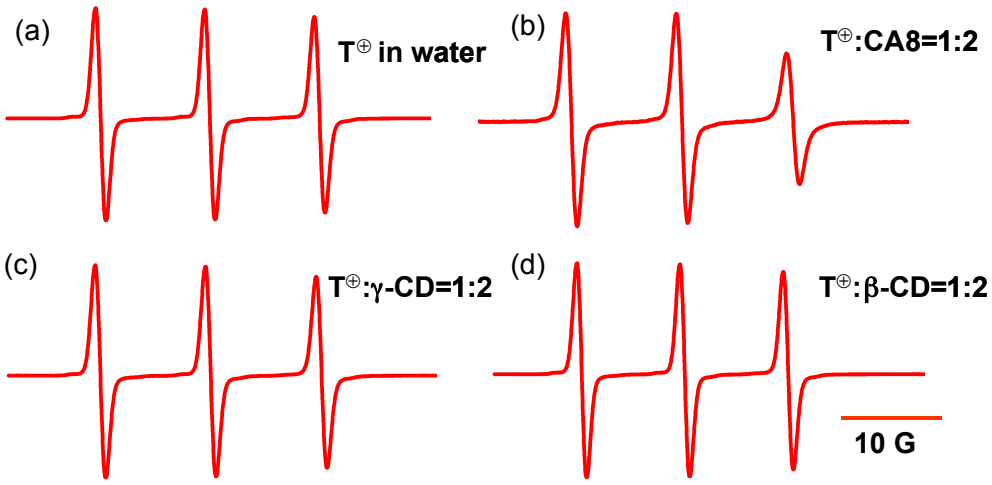


**Figure S5**. EPR spectra of (a) $\mathbf{T}^{\oplus}$ in water ($\tau_c$ = 0.02 ns, $A_N$ = 16.8 G), (b) $\mathbf{T}^{\oplus}$/CA8 (1:2) ($\tau_c$ = 0.17 ns, $A_N$ = 16.8 G), (c) $\mathbf{T}^{\oplus}$ /γ-CD (1:2) ($\tau_c$ = 0.02 ns, $A_N$ = 16.8 G) and (d) $\mathbf{T}^{\oplus}$ /β-CD ($\tau_c$ = 0.03 ns, $A_N$ = 16.8 G), [$\mathbf{T}^{\oplus}$] = 1mM, [CA8] = 2 mM, [γ-CD] = 2 mM and [β-CD] = 2 mM in 10 mM borate buffered $H_2O$.

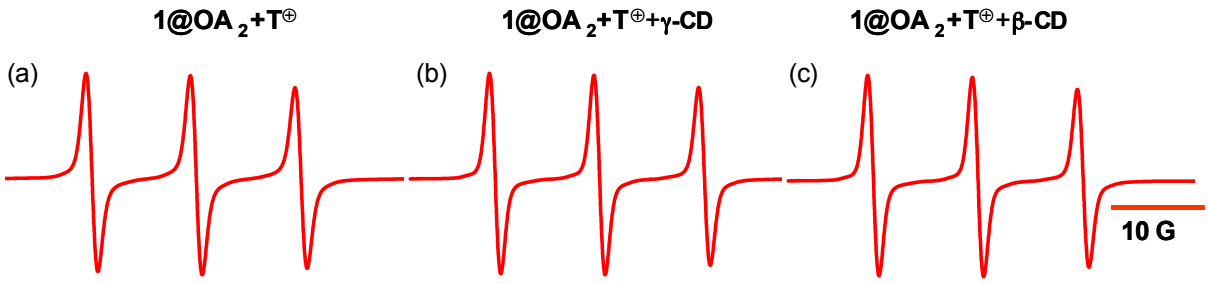


**Figure S6**. EPR spectra of (a) **1**/OA/ $\mathbf{T}^{\oplus}$ (1:2:2) ($\tau_c$ = 0.05 ns, $A_N$ = 16.7 G), (b) **1**/OA/$\mathbf{T}^{\oplus}$/γ-CD (1:2:2:2) ($\tau_c$ = 0.04 ns, $A_N$ = 16.8 G) and (c) **1**/OA/$\mathbf{T}^{\oplus}$/β-CD (1:2:2:2) ($\tau_c$ = 0.05 ns, $A_N$ = 16.7 G); [**1**] = 0.5 mM, [OA] = 1 mM, [$\mathbf{T}^{\oplus}$] = 1 mM, [γ-CD] = 1 mM, and [β-CD] = 1 mM in $H_2O$.

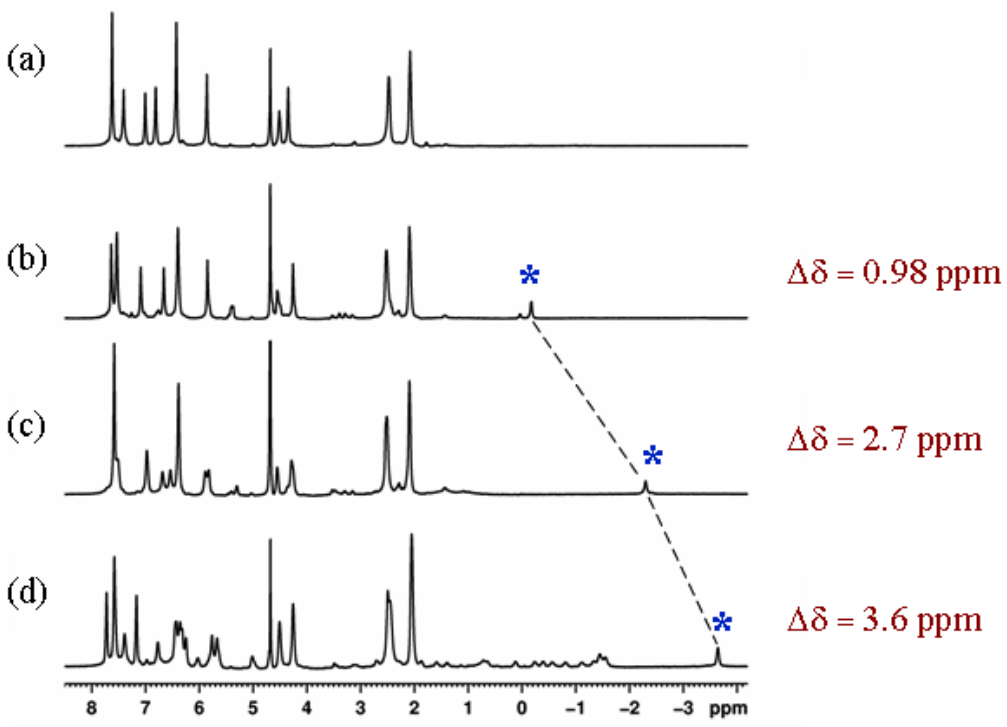


**Figure S7**. $^{1}$H NMR spectra (500 MHz, $D_2O$) of (a) OA, (b) α-methyl dibenzyl ketone @$OA_2$, (c) *para*-methyl dibenzyl ketone @$OA_2$ and (d) α-octyl dibenzyl ketone @$OA_2$; [guest] = 0.5 mM and [OA] = 1 mM in 10 mM borate buffered $D_2O$. "*" represents –$CH_3$ proton signals of corresponding guest molecule. Δδ is the difference in chemical shift in –$CH_3$ signal in $CDCl_3$ and inside OA capsule.

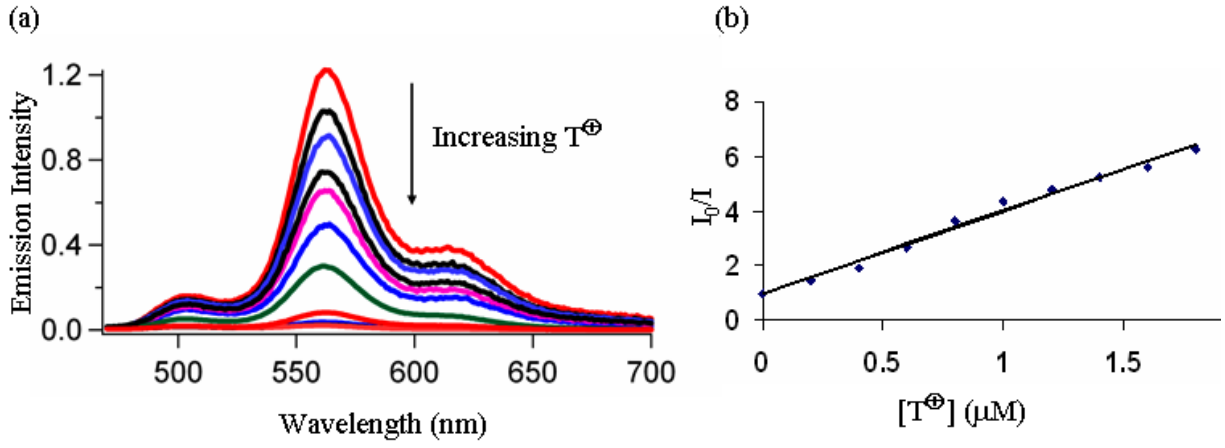


**Figure S8.** (a) Steady state phosphorescence titration of **1**@$OA_2$ with $\mathbf{T}^{\oplus}$and (b) Stern-Volmer plot for phosphorescence quenching of **1**@ $OA_2$ by $\mathbf{T}^{\oplus}$. $\lambda_{ex}$ = 320 nm, [**1**]= $1x10^{-5}$ M, [OA] = $2x10^{-5}$ M and [$\mathbf{T}^{\oplus}$] = 0 to 2 μM.

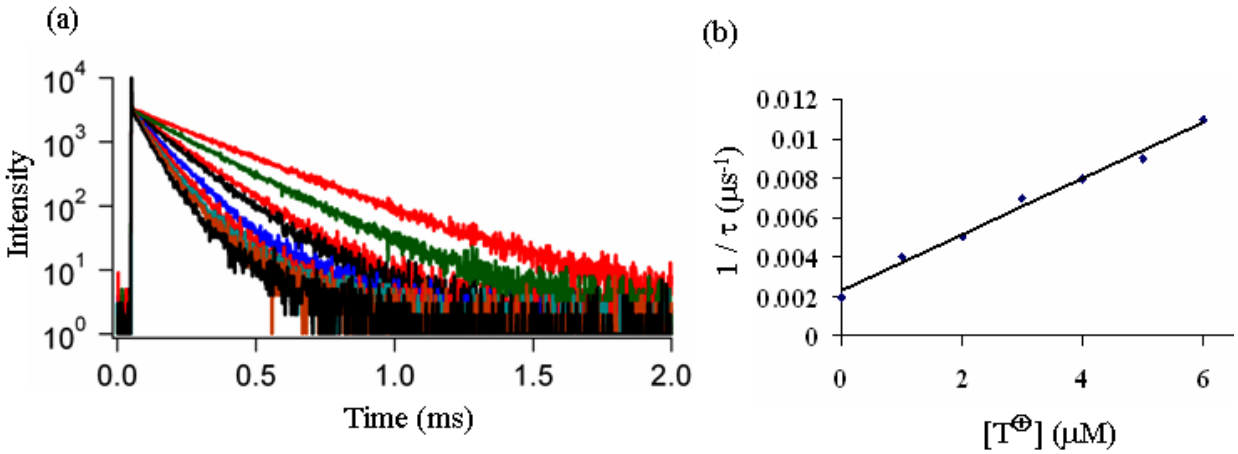


**Figure S9**. (a) Time resolved phosphorescence titration of **1**@$OA_2$ with $\mathbf{T}^{\oplus}$and (b) phosphorescence decay constant of **1**@$OA_2$ at different concentration of $\mathbf{T}^{\oplus}$. $\lambda_{ex}$ = 320 nm, $\lambda_{em}$ = 560 nm, [**1**]= $1x10^{-5}$ M, [OA] = $2x10^{-5}$ M and [$\mathbf{T}^{\oplus}$] = 0 to 6 μM; $k_q$ = (1.5±0.2) x $10^9$ $M^{-1}$ $s^{-1}$.

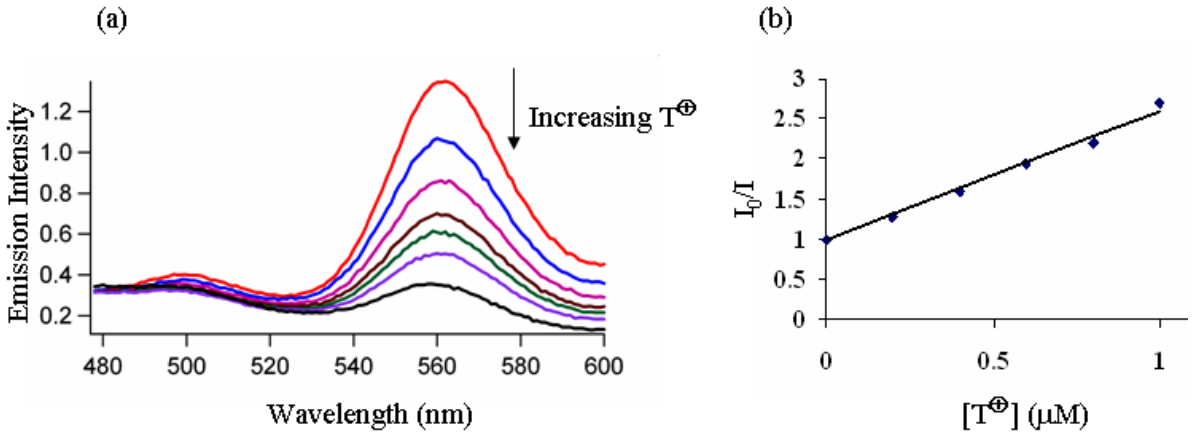


**Figure S10.** (a) Steady state phosphorescence titration of **2**@$OA_2$ with $\mathbf{T}^{\oplus}$and (b) Stern-Volmer plot for phosphorescence quenching of **2**@ $OA_2$ by $\mathbf{T}^{\oplus}$. $\lambda_{ex}$ = 300 nm, [**2**]= $1x10^{-5}$ M, [OA] = $2x10^{-5}$ M and [$\mathbf{T}^{\oplus}$] = 0 to 1 μM.

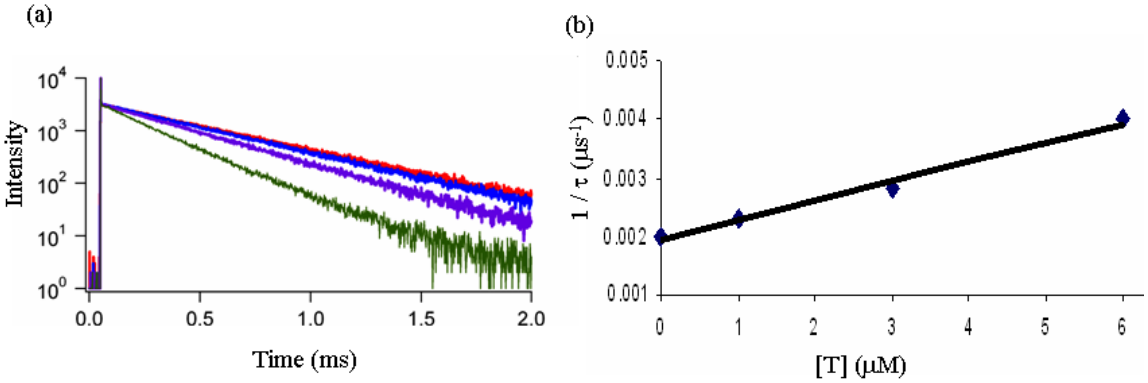


**Figure S11**. (a) Time resolved phosphorescence titration of **2**@$OA_2$ with $\mathbf{T}^{\oplus}$and (b) phosphorescence decay constant of **2**@$OA_2$ at different concentration of $\mathbf{T}^{\oplus}$. $\lambda_{ex}$ = 300 nm, $\lambda_{em}$ = 560 nm, [**1**]= $1x10^{-5}$ M, [OA] = $2x10^{-5}$ M and [$\mathbf{T}^{\oplus}$] = 0 to 1 μM; $k_q$ = (1.1±0.2) x $10^9$ $M^{-1}$ $s^{-1}$.

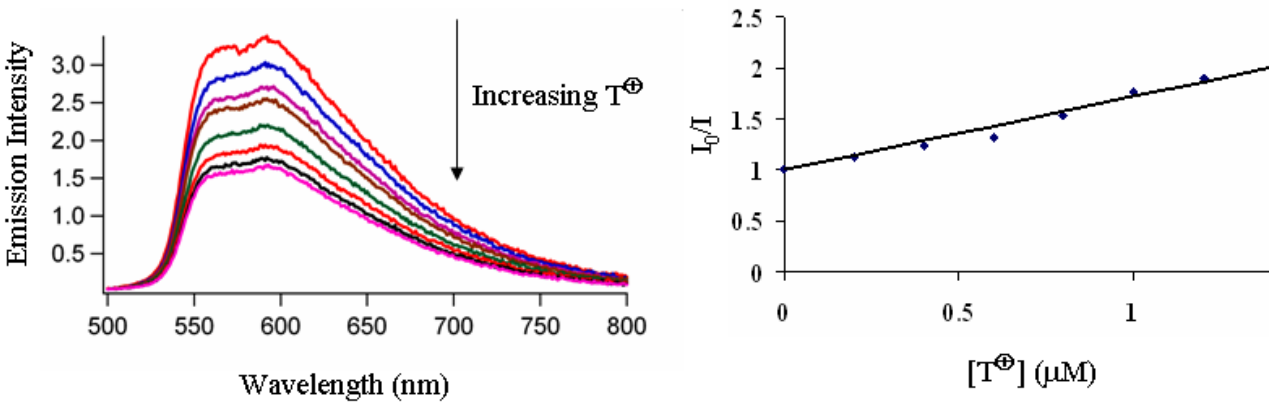


**Figure S12.** (a) Steady state phosphorescence titration of $\mathbf{3}_2$@$OA_2$ with $\mathbf{T}^{\oplus}$and (b) Stern-Volmer plot for phosphorescence quenching of $\mathbf{3}_2$@ $OA_2$ by $\mathbf{T}^{\oplus}$. $\lambda_{ex}$ = 254 nm, [**3**]= $2x10^{-5}$ M, [OA] = $2x10^{-5}$ M and [$\mathbf{T}^{\oplus}$] = 0 to 1.4 μM.

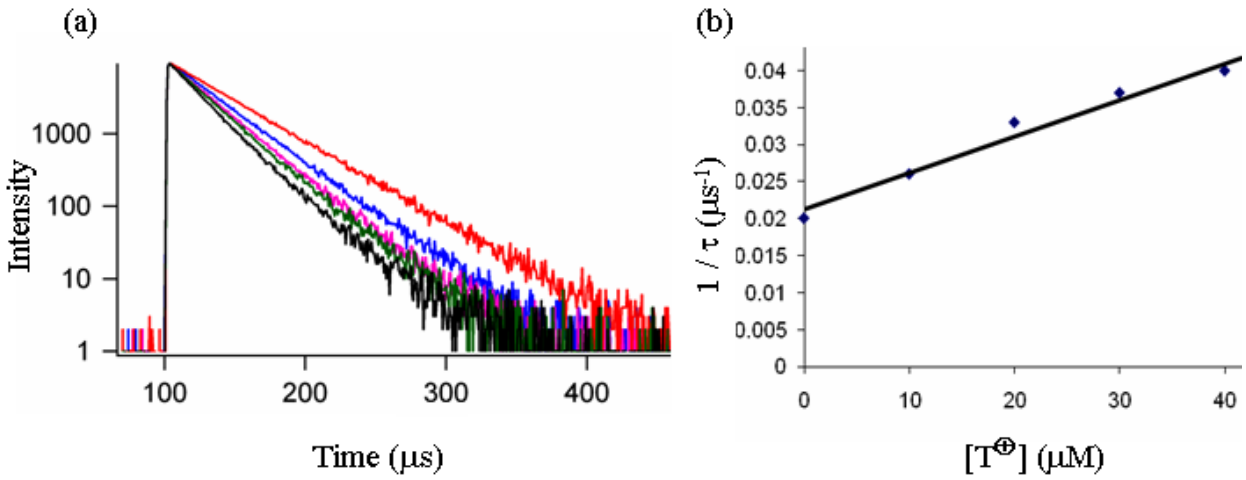


**Figure S13**. (a) Time resolved phosphorescence titration of $\mathbf{3}_2$@$OA_2$ with $\mathbf{T}^{\oplus}$and (b) phosphorescence decay constant of $\mathbf{3}_2$@$OA_2$ at different concentration of $\mathbf{T}^{\oplus}$. $\lambda_{ex}$ = 254 nm, $\lambda_{em}$ = 600 nm, [**3**]= $10^{-4}$ M, [OA] = $10^{-4}$ M and [$\mathbf{T}^{\oplus}$] = 0 to 50 μM, $k_q$ = (1±0.6) x $10^9$ $M^{-1}$ $s^{-1}$.

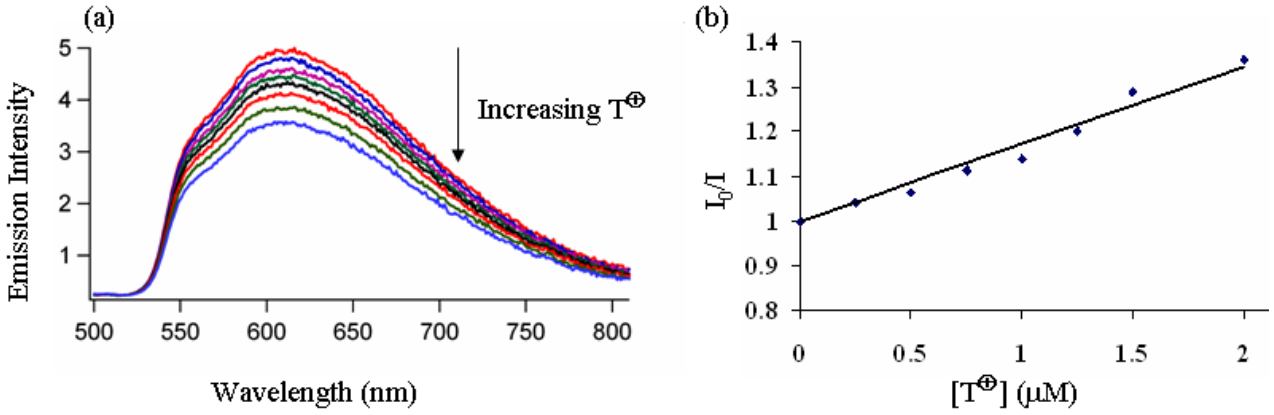


**Figure S14.** (a) Steady state phosphorescence titration of $\mathbf{4}_2$@$OA_2$ with $\mathbf{T}^{\oplus}$and (b) Stern-Volmer plot for phosphorescence quenching of $\mathbf{4}_2$@ $OA_2$ by $\mathbf{T}^{\oplus}$. $\lambda_{ex}$ = 254 nm, [**4**]= $2x10^{-5}$ M, [OA] = $2x10^{-5}$ M and [$\mathbf{T}^{\oplus}$] = 0 to 2 μM.

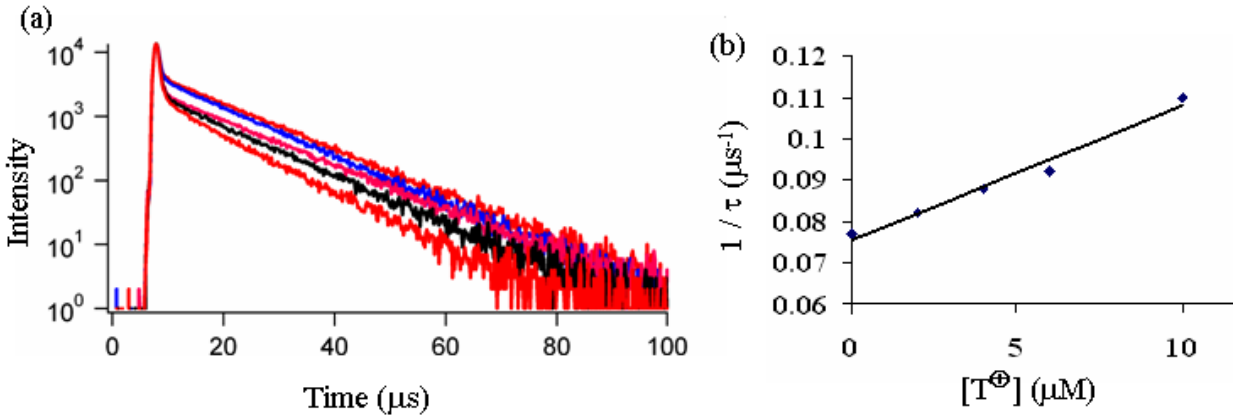


**Figure S15**. (a) Time resolved phosphorescence titration of $\mathbf{4}_2$@$OA_2$ with $\mathbf{T}^{\oplus}$and (b) phosphorescence decay constant of $\mathbf{4}_2$@$OA_2$ at different concentration of $\mathbf{T}^{\oplus}$. $\lambda_{ex}$ = 254 nm, $\lambda_{em}$ = 600 nm, [**4**]= $2x10^{-5}$ M, [OA] = $2x10^{-5}$ M and [$\mathbf{T}^{\oplus}$] = 0 to 10 μM; $k_q$ = (2±0.5) x $10^9$ $M^{-1}$ $s^{-1}$.

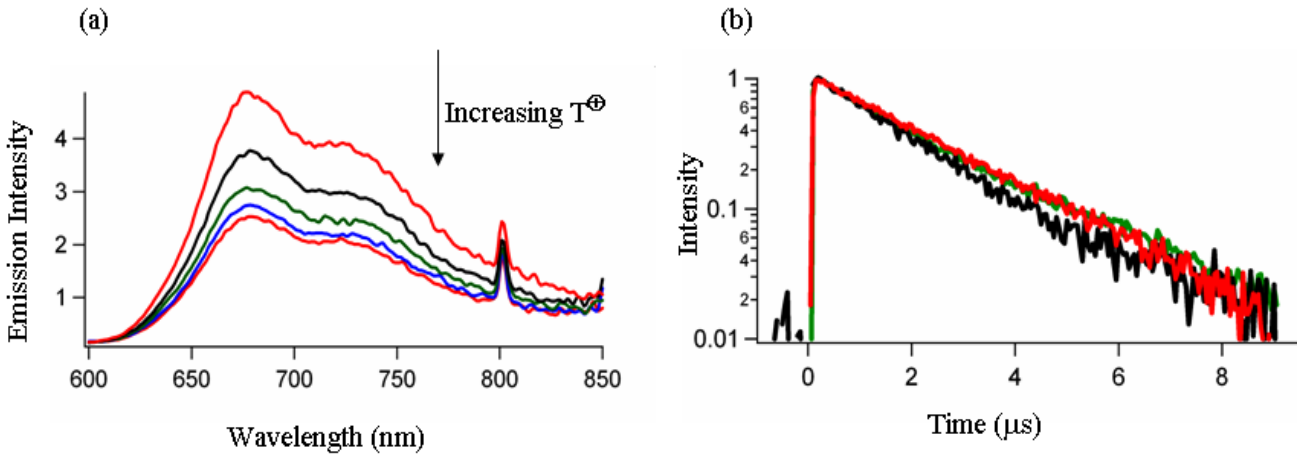


**Figure S16.** (a) Steady state phosphorescence titration of **5**@$OA_2$ with $\mathbf{T}^{\oplus}$ and (b) time resolved phosphorescence titration of **5**@$OA_2$ with $T^{\oplus}$. $\lambda_{ex}$ = 400 nm, $\lambda_{em}$ = 675 nm, [**5**]= $1x10^{-5}$ M, [OA] = $2x10^{-5}$ M and [$\mathbf{T}^{\oplus}$] = 0 to 10 μM.

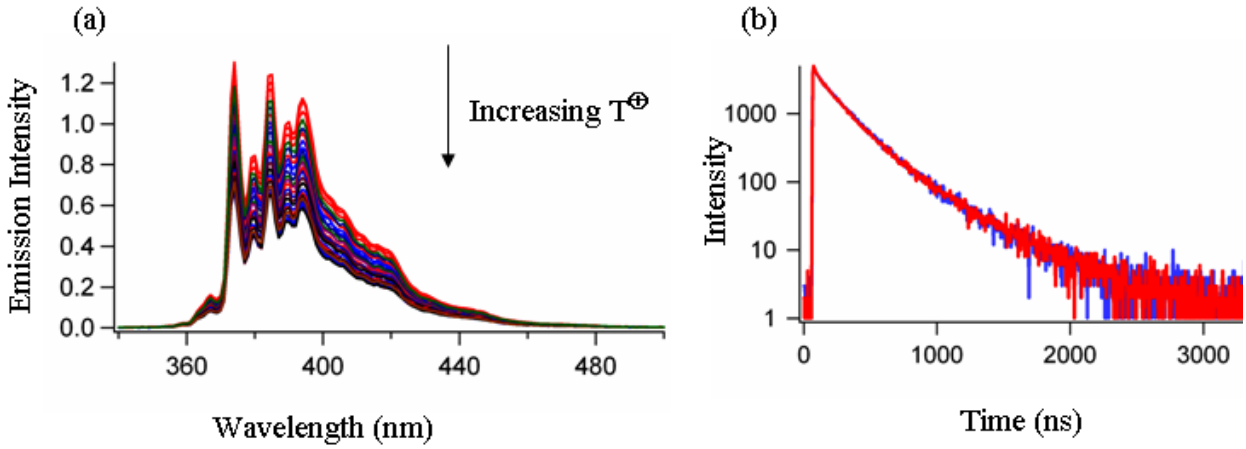


**Figure S17.** (a) Steady state fluorescence titration of **6**@$OA_2$ with $\mathbf{T}^{\oplus}$and (b) time resolved phosphorescence titration of **6**@$OA_2$ with $T^{\oplus}$. $\lambda_{ex}$ = 320 nm, $\lambda_{em}$ = 375 nm, [**6**]= $1x10^{-5}$ M, [OA] = $2x10^{-5}$ M and [$\mathbf{T}^{\oplus}$] = 0 to 20 μM.

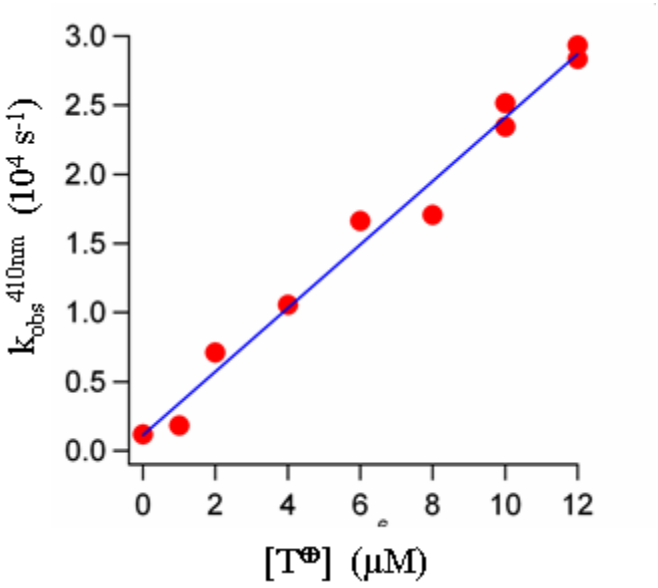


**Figure S18**. Time resolved triplet-triplet absorption titration of **6**@$OA_2$ with $\mathbf{T}^{\oplus}$; $k_q$ = (2.3±0.1) x $10^9$ $M^{-1}$ $s^{-1}$, [**6**] = 4 x$10^{-5}$ M, [OA] = 8x$10^{-5}$ M, [$\mathbf{T}^{\oplus}$] = 0 to 12 μM

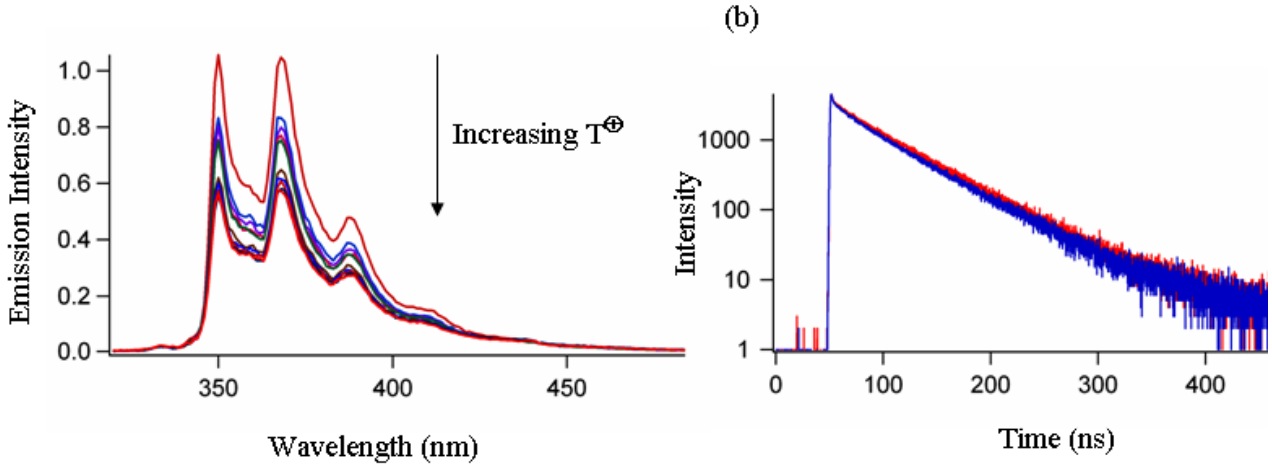


**Figure S19.** (a) Steady state fluorescence titration of **7**@$OA_2$ with $\mathbf{T}^{\oplus}$and (b) time resolved phosphorescence quenching of **7**@ $OA_2$ by $\mathbf{T}^{\oplus}$. $\lambda_{ex}$ = 300 nm, $\lambda_{em}$ = 350 nm, [**7**]= 1x$10^{-5}$ M, [OA] = 2x$10^{-5}$ M and [$\mathbf{T}^{\oplus}$] = 0 to 20 μM.

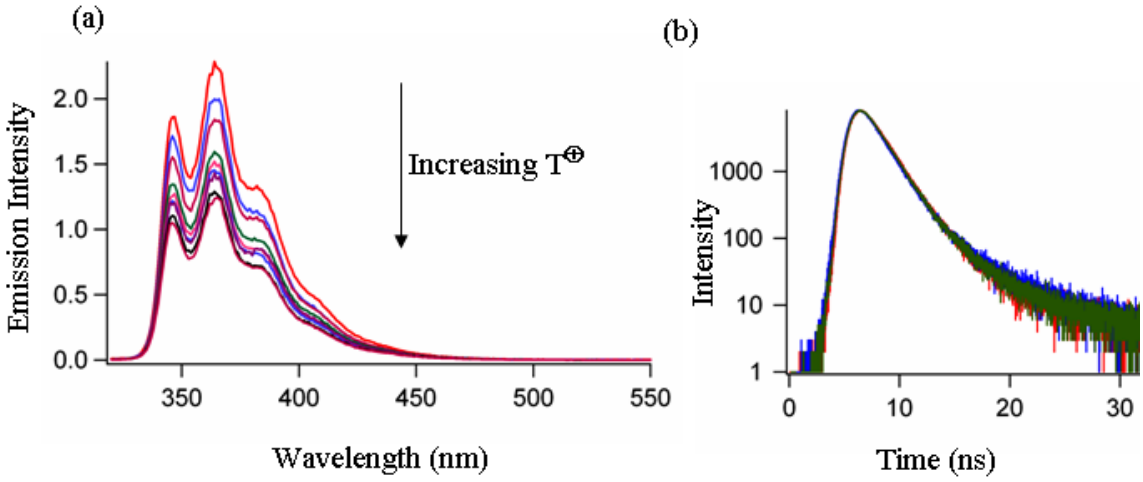


**Figure S20.** (a) Steady state fluorescence titration of **8**@$OA_2$ with $\mathbf{T}^{\oplus}$ and (b) time resolved fluorescence titration of **8**@$OA_2$ with $T^{\oplus}$. $\lambda_{ex}$ = 320 nm, $\lambda_{em}$ = 350 nm, [**8**]= $1x10^{-5}$ M, [OA] = $2x10^{-5}$ M and [$\mathbf{T}^{\oplus}$] = 0 to 20 μM.

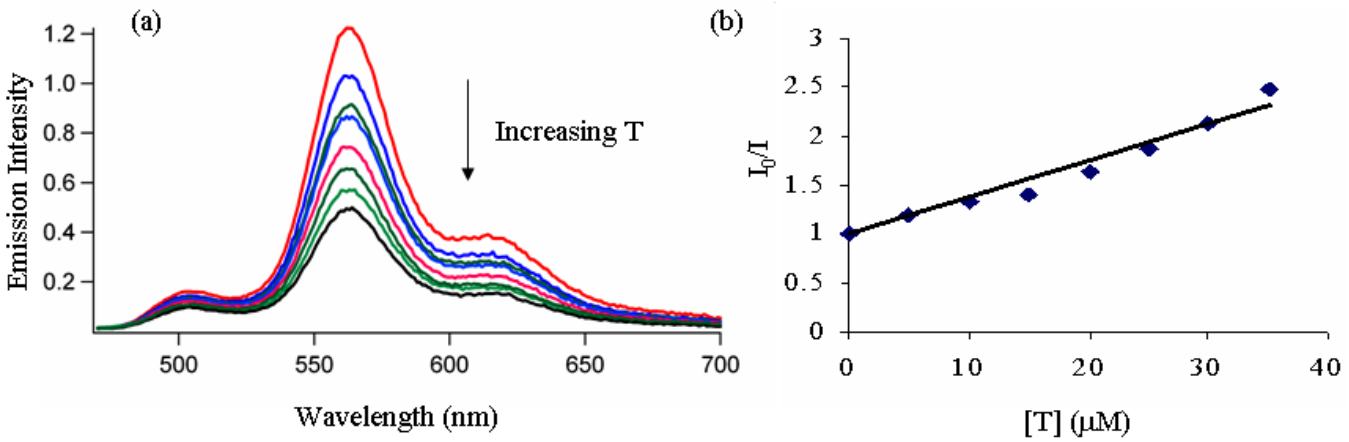


**Figure S21.** (a) Steady state phosphorescence titration of **1**@$OA_2$ with **T** and (b) Stern-Volmer plot for phosphorescence quenching of **1**@ $OA_2$ by **T**. $\lambda_{ex}$ = 320 nm, [**1**]= $1x10^{-5}$ M, [OA] = $2x10^{-5}$ M and [**T**] = 0 to 35 μM.

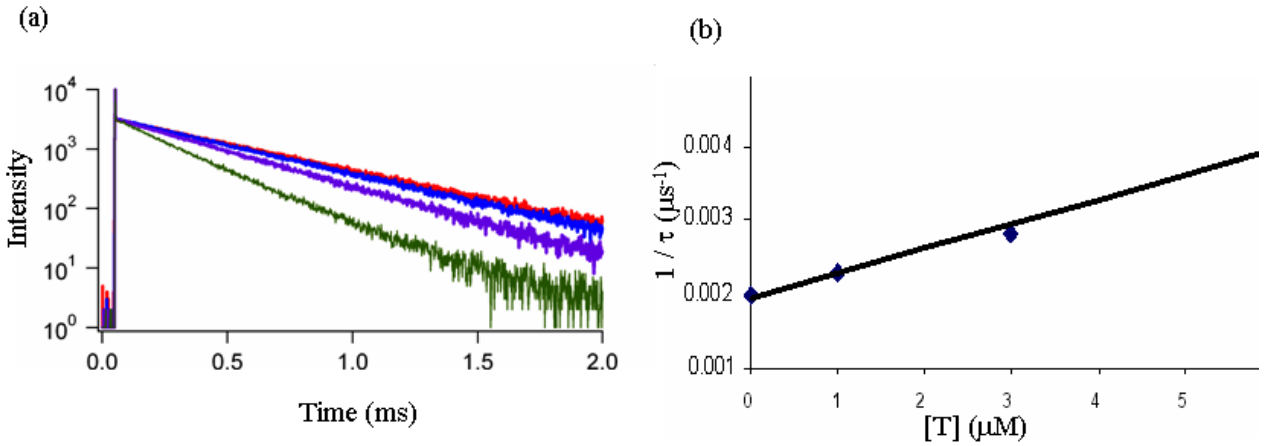


**Figure S22**. (a) Time resolved phosphorescence titration of **1**@$OA_2$ with **T** and (b) phosphorescence decay constant of **1**@$OA_2$ at different concentration of **T**. $\lambda_{ex}$ = 320 nm, $\lambda_{em}$ = 560 nm, [**1**]= 1x$10^{-5}$ M, [OA] = 2x$10^{-5}$ M and [**T**] = 0 to 6 μM; $k_q$ = (2±1) x $10^8$ $M^{-1}$ $s^{-1}$.

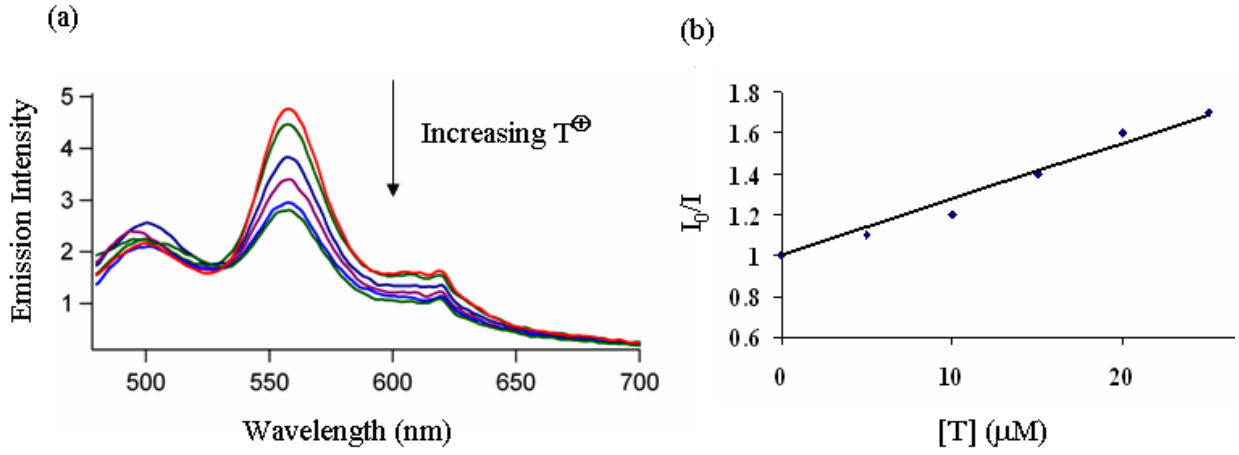


**Figure S23.** (a) Steady state phosphorescence titration of **2**@$OA_2$ with **T** and (b) Stern-Volmer plot for phosphorescence quenching of **2**@ $OA_2$ by **T**. $\lambda_{ex}$ = 320 nm, [**2**]= 1x$10^{-5}$ M, [OA] = 2x$10^{-5}$ M and [**T**] = 0 to 25 μM.

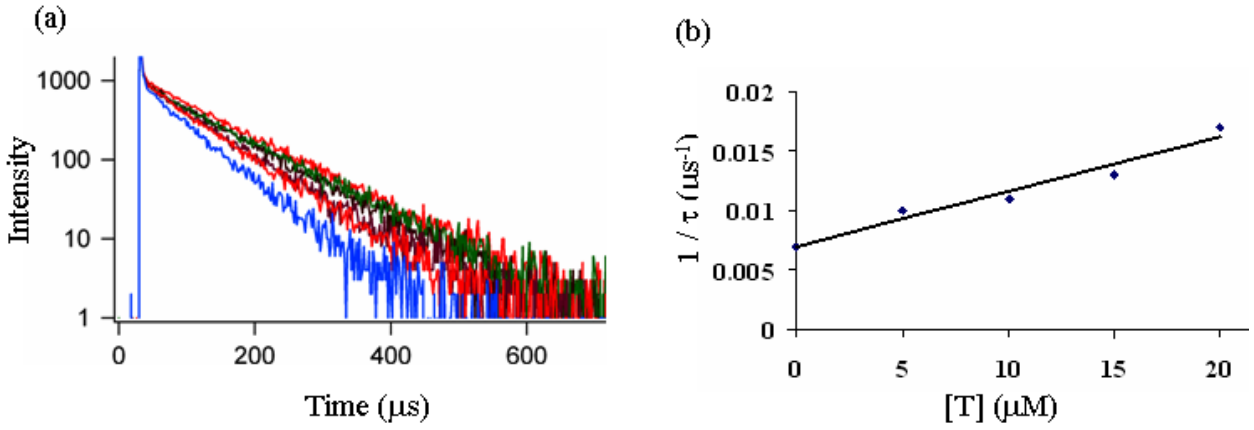


**Figure S24**. (a) Time resolved phosphorescence titration of **2**@$OA_2$ with **T** and (b) phosphorescence decay constant of **2**@$OA_2$ at different concentration of **T**. $\lambda_{ex}$ = 320 nm, $\lambda_{em}$ = 560 nm, [**2**]= $1x10^{-5}$ M, [OA] = $2x10^{-5}$ M and [**T**] = 0 to 20 μM; $k_q$ = (4±0.8) x $10^7$ $M^{-1}$ $s^{-1}$

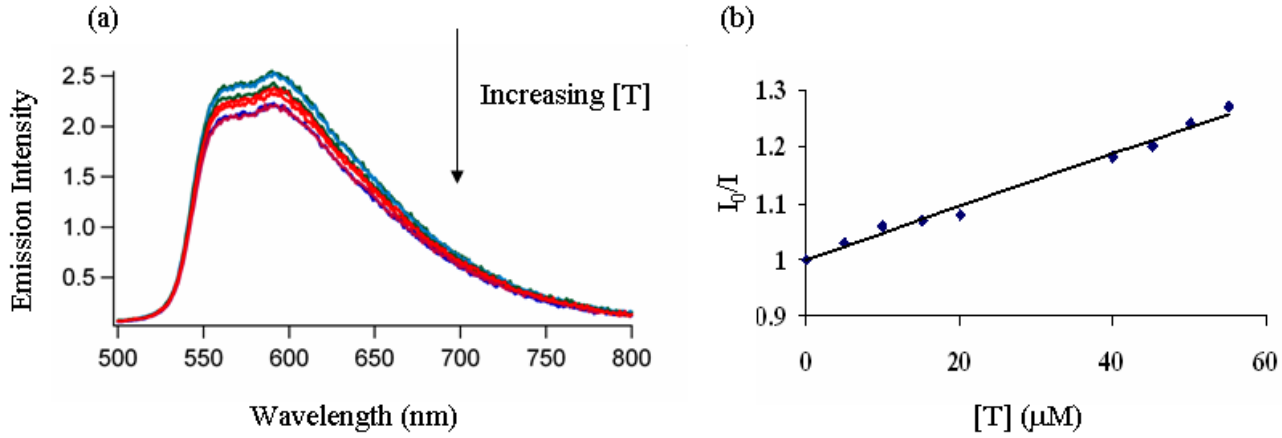


**Figure S25.** (a) Steady state phosphorescence titration of $\mathbf{3}_2$@$OA_2$ with **T** and (b) Stern-Volmer plot for phosphorescence quenching of $\mathbf{3}_2$@ $OA_2$ by **T**. $\lambda_{ex}$ = 254 nm, [**3**]= $2x10^{-5}$ M, [OA] = $2x10^{-5}$ M and [**T**] = 0 to 60 μM.

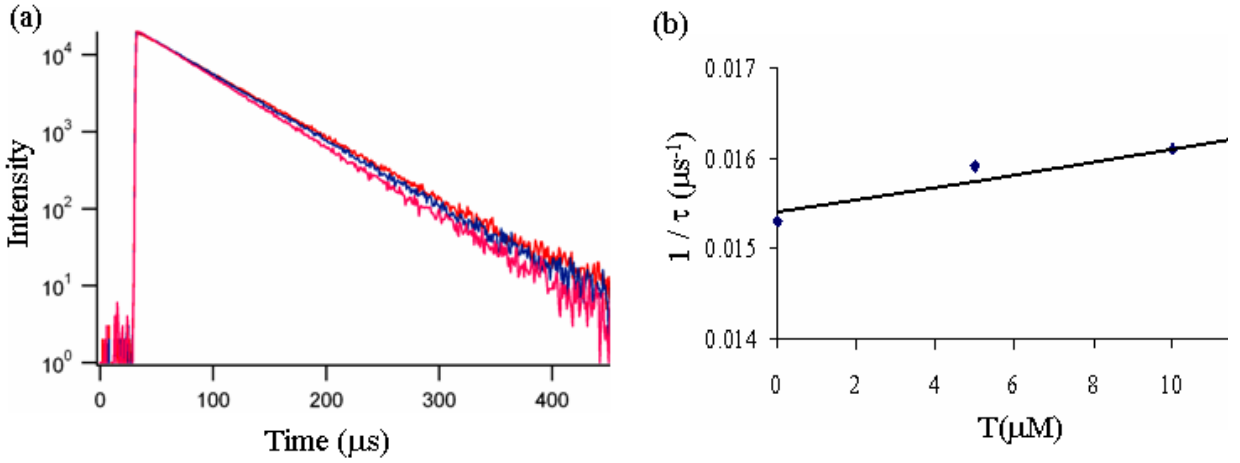


**Figure S26**. (a) Time resolved phosphorescence titration of $\mathbf{3}_2$@$OA_2$ with **T** and (b) phosphorescence decay constant of $\mathbf{3}_2$@$OA_2$ at different concentration of **T.** $\lambda_{ex}$ = 254 nm, $\lambda_{em}$ = 600 nm, [**3**]= $2x10^{-5}$ M, [OA] = $2x10^{-5}$ M and [**T**] = 0 to 10 μM, $k_q$ = (7±2) x $10^7$ $M^{-1}$ $s^{-1}$.

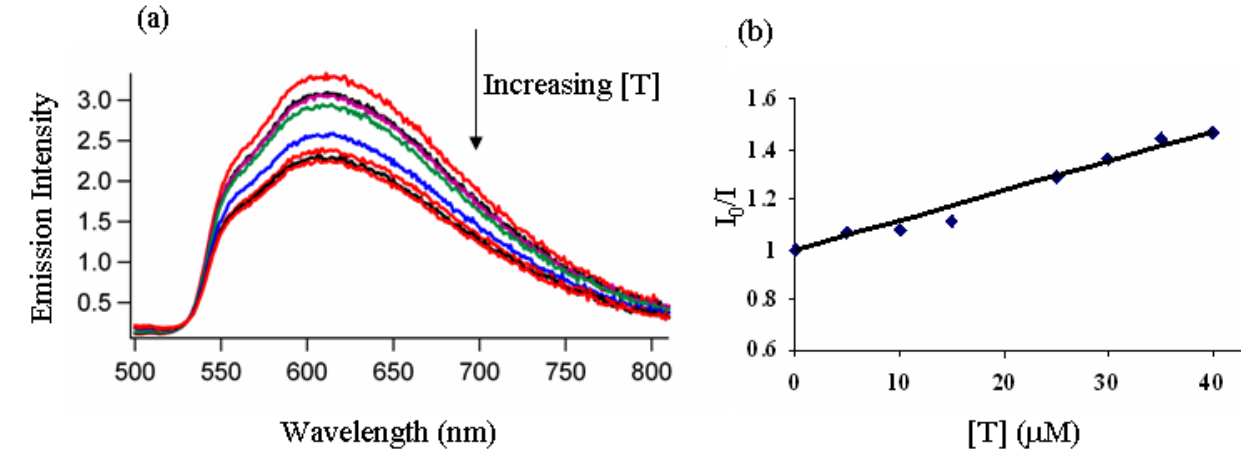


**Figure S27.** (a) Steady state phosphorescence titration of $\mathbf{4}_2$@$OA_2$ with **T** and (b) Stern-Volmer plot for phosphorescence quenching of $\mathbf{4}_2$@ $OA_2$ by **T**. $\lambda_{ex}$ = 254 nm, [**4**]= $2x10^{-5}$ M, [OA] = $2x10^{-5}$ M and [**T**] = 0 to 40 μM.

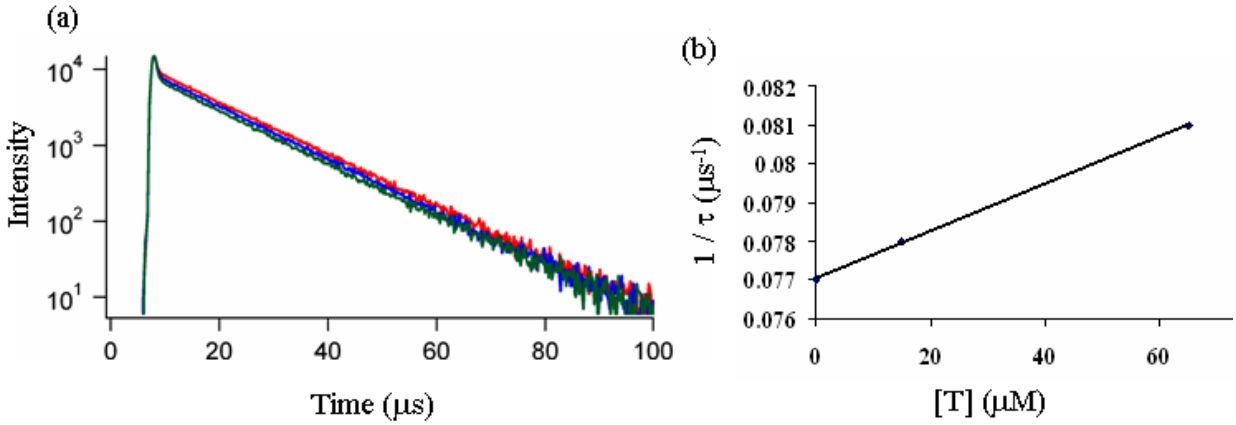


**Figure S28**. (a) Time resolved phosphorescence titration of $\mathbf{4}_2$@$OA_2$ with **T** and (b) phosphorescence decay constant of $\mathbf{4}_2$@$OA_2$ at different concentration of **T.** $\lambda_{ex}$ = 254 nm, $\lambda_{em}$ = 625 nm, [**4**] = 2x10$^{-5}$ M, [OA] = 2x10$^{-5}$ M and [**T**] = 0 to 65 μM; $k_q$ = (6±2) x 10$^7$ M$^{-1}$ s$^{-1}$.

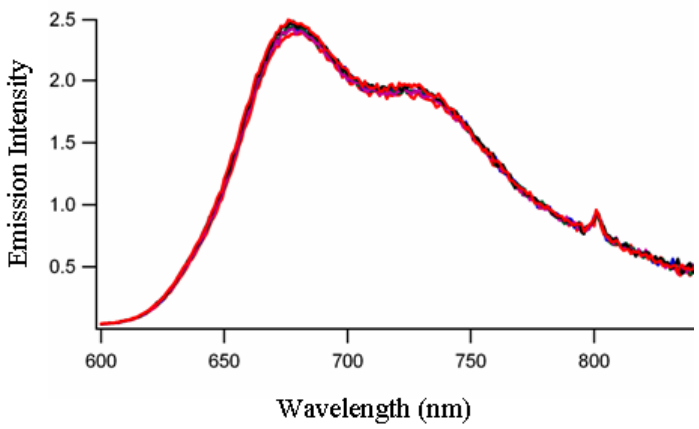


**Figure S29.** Steady state phosphorescence titration of **5**@$OA_2$ with **T.** $\lambda_{ex}$ = 400 nm, [**1**]= 1x10$^{-5}$ M, [OA] = 2x10$^{-5}$ M and [**T**] = 0 to 50 μM.

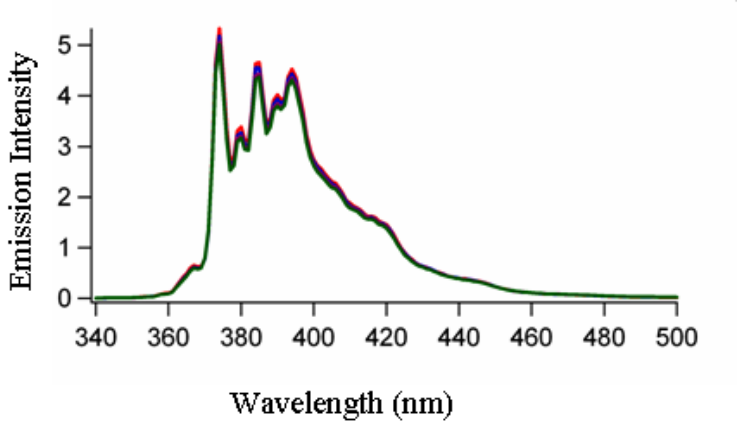


**Figure S30.** Steady state fluorescence titration of **6**@$OA_2$ with **T**. $\lambda_{ex}$ = 320 nm, [**1**]= $1x10^{-5}$ M, [OA] = $2x10^{-5}$ M and [**T**] = 0 to 50 μM.

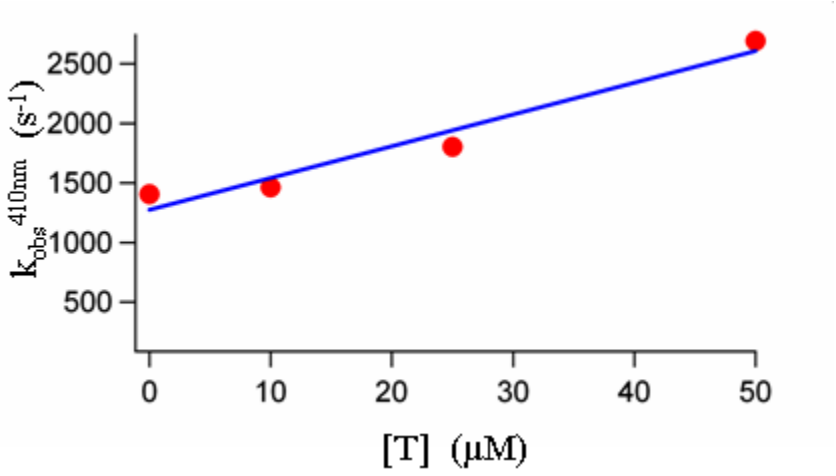


**Figure S31**. Time resolved triplet-triplet absorption titration of **6**@$OA_2$ with **T**, [**6**]= $4x10^{-5}$ M, [OA] = $8x10^{-5}$ M and [**T**] = 0 to 80 μM; $k_q$ = (1.6±0.5) x $10^7$ $M^{-1}$ $s^{-1}$.

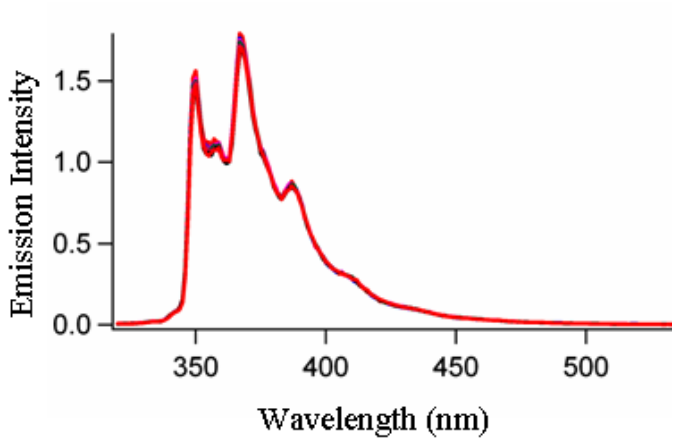


**Figure S32.** Steady state fluorescence titration of **7**@$OA_2$ with **T**. $\lambda_{ex}$ = 300 nm, [**7**]= $1x10^{-5}$ M, [OA] = $2x10^{-5}$ M and [**T**] = 0 to 50 μM.

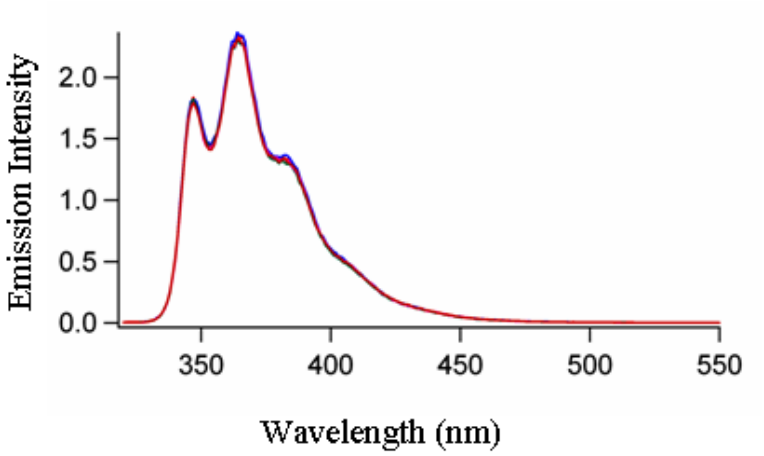


**Figure S33.** Steady state fluorescence titration of **8**@$OA_2$ with **T.** $\lambda_{ex}$ = 300 nm, [**8**]= $1x10^{-5}$ M, [OA] = $2x10^{-5}$ M and [**T**] = 0 to 50 μM.

**Table S1**. $^1$H relaxation time ($T_1$) for OA (host) and **1** (guest) in presence of nitroxide radicals ($T^{\oplus}$, T and $T^{\ominus}$, see Scheme S1).

| Protons | $(T_{1,d})^a$ | $(T_{1,obs})^b$ $[T^{\oplus}]$ | $(1/T_{1,p})^c$ $[T^{\oplus}]$ | $(T_{1,obs})$ [T] | $(1/T_{1,p})$ [T] | $(T_{1,obs})$ $[T^{\ominus}]$ | $(1/T_{1,p})$ $[T^{\ominus}]$ |
|---|---|---|---|---|---|---|---|
| $H_A$ | 2.42 | 0.07 | 14.28 | 0.31 | 2.86 | 2.09 | 0.07 |
| $H_B$ | 0.56 | 0.23 | 2.56 | 0.32 | 1.33 | 0.54 | 0.07 |
| $H_C$ | 0.76 | 0.08 | 11.11 | 0.24 | 2.86 | 0.7 | 0.11 |
| $H_D$ | 0.35 | 0.15 | 2.85 | 0.19 | 2.38 | 0.31 | 0.37 |
| $H_E$ | 1.14 | 0.14 | 6.25 | 0.31 | 2.33 | 0.96 | 0.16 |
| $H_F$ | 1.11 | 0.14 | 6.25 | 0.3 | 2.44 | 0.88 | 0.24 |
| $H_I$ | 0.38 | 0.19 | 2.63 | 0.26 | 1.22 | 0.36 | 0.15 |
| $H_J$ | 0.35 | 0.12 | 5.56 | 0.23 | 1.49 | 0.32 | 0.26 |
| $H_{-CH3}$ | 0.82 | 0.38 | 1.43 | 0.5 | 0.78 | 0.78 | 0.06 |

Note:

[a] $T_{1,d}$ = relaxation time in absence of the paramagnetic center

[b] $T_{1,obs}$= observed relaxation time in presence of paramagnetic center

[c] $T_{1,p}$= relaxation time caused by the paramagnetic species

$1/T_{1,p} = 1/T_{1,obs} - 1/T_{1,d}$

$1/T_{1,p} \propto r^{-6}$, r = distance between nucleus and paramagnetic center.

[**1**] = 0.5 mM, [OA] = 1 mM, [$\mathbf{T}^{\oplus}$] = [**T**] = [$\mathbf{T}^{\ominus}$] = 0.5 mM, in 10 mM borate buffered $D_2O$.

Relaxation time for $H_G$ and $H_H$ could not be measured as these proton signals merged with residual $H_2O$ signal.

**Table S2**. $^1$H relaxation time ($T_1$) for OA (host) and **1** (guest) in presence of $T^{\oplus}$ (see Scheme 1) and other hosts (CB8, CA8 and γ-CD)

| Protons | $(T_{1,d})^a$ | $(T_{1,obs})^b$ $[T^{\oplus}]$ + CB8 | $(T_{1,p})^c$ $[T^{\oplus}]$ + CB8 | $(T_{1,obs})$ $[T^{\oplus}]$+ CA8 | $(T_{1,p})$ $[T^{\oplus}]$ + CA8 | $(T_{1,obs})$ $[T^{\oplus}]$+ γ-CD | $(T_{1,p})$ $[T^{\oplus}]$ + γ-CD |
|---|---|---|---|---|---|---|---|
| $H_A$ | 2.42 | 1.64 | 0.2 | 1 | 0.6 | 0.15 | 6.26 |
| $H_B$ | 0.56 | 0.52 | 0.13 | 0.4 | 0.71 | 0.26 | 2.06 |
| $H_C$ | 0.76 | 0.68 | 0.15 | 0.66 | 0.2 | 0.05 | 18.68 |
| $H_D$ | 0.35 | 0.35 | 0.03 | 0.26 | 0.99 | 0.13 | 4.83 |
| $H_E$ | 1.14 | 1.06 | 0.07 | 1.14 | 0 | 0.15 | 5.79 |
| $H_F$ | 1.11 | 1.05 | 0.05 | 1.1 | 0.01 | 0.28 | 2.67 |
| $H_I$ | 0.38 | 0.35 | 0.2 | 0.3 | 0.7 | 0.27 | 1.07 |
| $H_J$ | 0.35 | 0.35 | 0 | 0.29 | 0.6 | 0.1 | 7.14 |
| $H_{-CH3}$ | 0.82 | 0.76 | 0.09 | 0.79 | 0.05 | 0.37 | 1.48 |

Note:

[a] $T_{1,d}$ = relaxation time in absence of the paramagnetic center

[b] $T_{1,obs}$ = observed relaxation time in presence of paramagnetic center and other host

[c] $T_{1,p}$ = relaxation time caused by the paramagnetic species in presence of other host

$1/T_{1,p} = 1/T_{1,obs} - 1/T_{1,d}$

$1/T_{1,p} \propto r^{-6}$, r = distance between nucleus and paramagnetic center.

[**1**] = 0.5 mM, [OA] = 1 mM, [$\mathbf{T}^{\oplus}$] = 0.5 mM, [CB8] =0.5 mM, [CA8] = 0.5 mM and [γ-CD] = 0.5 mM in 10 mM borate buffered $D_2O$.

Relaxation time for $H_G$ and $H_H$ could not be measured as these proton signals merged with residual $H_2O$ signal.

**Experimental Section**

*Materials and Methods:* Guests 4,4'-dimethylbenzil (**1**), benzil (**2**), 4-carboxy-TEMPO ($T^{\ominus}$) and TEMPO (T) were used as received from Sigma-Aldrich/Acros. Camphorthione[1] (**3**), adamantanethione[1] (**4**), xanthione[1] (**5**), 4,4'-dimethyl stilbene[2] (**8**) and cationic nitroxide radical ($T^{\oplus}$)[3] were synthesized following literature procedures. Pyrene (**6**) and phenanthrene (**7**) (from Sigma-Aldrich/Acros) were recrystallized from EtOH. The hosts octa acid[4], cucurbit[7]uril[5], calixarene octasulfonic acid[6,7] were synthesized following published procedures. β-cyclodextrin and γ-cyclodextrin were purchased from Sigma-Aldrich/Acros.

*General protocol for NMR study:*

$^1$H NMR studies were carried out on a Bruker 500 MHz NMR spectrometer at 25 °C. 600 μL of a $D_2O$ solution of host OA (1mM OA in 10 mM $Na_2B_4O_7$) was taken in a NMR tube and to this 0.5 equivalent increment of guest (5 μL of a 60 mM solution in DMSO-$d_6$) was added. The $^1$H NMR experiments were carried out after shaking the NMR tube for 5 min after each addition. Completion of complexation was monitored by disappearance of the free host OA signals upon addition of guest. Required amount of nitroxide solution ($T^{\oplus}$, T and $T^{\ominus}$; stock solutions (30 mM) were prepared in $D_2O$) was added in the complex and $^1$H NMR was recorded after shaking the NMR tube for 5 min. Spin-lattice relaxation times $T_1$ were determined using a standard 180-τ-90 inversion recovery pulse sequence with 10 τ values between 0.001 to 10 s. The $T_1$ measurements were performed on a Bruker 400 MHz NMR spectrometer at 25 °C.

*General protocol for luminescence study:*

Fluorescence emission spectra were recorded on a FS920CDT Edinburgh steady-state fluorimeter and the lifetime measurements on FL900CDT fluorescence lifetime spectrometer. Capsular assemblies (1 mM) were made by adding 5 μL (for 2:1; H:G complex) and 10 μL (for 2:2; H:G complex) of 60 mM solution of guest (in DMSO solution) to 0.6 mL of 1mM OA in 10 mM borate buffer in $H_2O$. It was diluted appropriately with 10 mM buffer solution to have the required concentration of host/guest complex. The solutions were deoxygenated by purging with nitrogen gas for 30 min prior

to the emission study. 10 μL of nitroxides ($T^{\oplus}$, T and $T^{\ominus}$; stock solutions were prepared in $H_2O$) were added each time and further deoxygenated by purging nitrogen for 20 min and then recorded emission spectra. The quenching rate constants for nitroxide quenching were derived from the slope of the plot of nitroxide concentration vs. triplet state decay constant ($1/\tau$). Required amount of CB8 (stock solution was prepared in $H_2O$) was added to the solution (after quenching by nitroxide) and emission spectra were recorded after purging with nitrogen.

*Triplet-triplet absorption measurements:*

Transient absorption measurements were performed by laser flash photolysis employing the pulses from a Nd-YAG laser (GCR-150-30, Spectra Physics) at 355 nm (~5 ns pulse length) and a computer-controlled system that has been described elsewhere.[10]

*General protocol for EPR study:*

*Preparation of host/guest complex:* Stock solution (20 mM) of guest was prepared in $CHCl_3$. Host stock solution (5 mM) was prepared in $H_2O$. Required amount of guest solution in $CHCl_3$ was added in a vial and the solvent was evaporated by shaking in a mechanical shaker. Then calculated amount of host solution and water were added and shaken by the mechanical shaker for 15 h. The required amount of nitroxide solutions were added to it and shaken for 2 h.

EPR spectra were recorded at room temperature in Bruker EMX spectrometer at 9.5 GHz (X band) employing 100 KHz of field modulation frequency. Spectrometer setting:
Power, 1.997 mW; amplitude modulation, 0.50 G; time constant, 163.84 ms; conversion time, 163.84 ms. Samples were loaded to quartz (CFQ) EPR tubes from Wilmad LabGlass (2 mm OD, 0.5 mm wall thickness, 10 cm height) for the EPR experiments.

*EPR Simulations:*

The EPR spectra of three-line signals (three hyperfine lines: $2I_N+1 = 3$) were computed by the well-established procedure of Budil and Freed.[8] The main input parameters were as follows. (a) the $g_{ii}$ components (for the coupling between the electron spin and the

magnetic field) were the ones previously used for the nitroxide ($g_{xx}$=2.009, $g_{yy}$=2.006, $g_{zz}$=2.0025),[9] and were considered constant for all samples; (b) The $A_{ii}$ principal values of the **A** tensor for the coupling between electron and nuclear spin ($<A_N>=(A_{xx}+A_{yy}+A_{zz})/3$). An increase in the environmental polarity of the NO group provokes an increase in the **A** tensor components owing to the increased electron spin density on the nitrogen nucleus. (c) The perpendicular component of the correlation time for rotational diffusion ($\tau_{perp}$). Brownian motion was assumed in the calculation, for which the diffusion component is $D_{perp} = 1/(6\tau_{perp})$. The EPR spectra of the seven-line signal were computed by using the program Simfonia by Bruker.

*References:*


[1] Jayaraj, N.; Jockusch, S.; Kaanumalle, L. S.; Turro, N. J.; Ramamurthy, V. *Can. J. Chem.* **2011,** *89,* 203-213.

[2] Parthasarathy, A.; Ramamurthy, V. *Photochem. Photobiol. Sci.* **2011,** Advanced Article.

[3] Jayaraj, N.; Porel, M.; Ottaviani, F. M.; Maddipatla, M. V. S.; Modelli, A., Da Silva, J.; Bhogala, B. R.; Captain, B.; Jockusch, S.; Turro, N. J.; Ramamurthy, V. *Langmuir*, **2009**, *25*,13820–13832

[4] Gibb, C. L. D.; Gibb, B. C. *J. Am. Chem. Soc.* **2004**, *126*, 11408–11409.

[5] Day, A.; Arnold, A. P.; Blanch, R. J.; Snushall, B. *J. Org. Chem.* **2001**, *66*, 8094.

[6] Gutsche, C. D.; Dhawan, B.; No, K. H.; Muthukrishnan, R. *J. Am. Chem. Soc.,* **1981**, *103*, 3782-3792.

[7] Shinkai, S.; Mori, S.; Koreishi, H.; Tsubaki, T.; Manabe, O.; *J. Am. Chem. Soc*., **1986**, *108*, 2409-2416.

[8] Budil, D. E.; Lee, S.; Saxena, S.; Freed, J. H. *J. Magn. Reson.,* **1996**, *A120*, 155.

[9] Klajnert, B.; Cangiotti, M.; Calici, S.; Majoral, J.P.; Caminade, A.M.; Cladera, J.; Bryszewska, M.; Ottaviani, M.F. *Macromolec. Biosci.,* **2007**, *7*, 1065-1074.

[10] Yagci, Y.; Jockusch, S.; Turro, N. J. *Macromolecules*, **2007**, *40*, 4481-4485